Phase behavior of the Lattice Restricted Primitive Model with nearest-neighbor exclusion

Alexandre Diehl
Departamento de Física, Universidade Federal do Ceará, Caixa Postal 6030, CEP 60455-760, Fortaleza, CE, Brazil

Athanassios Z. Panagiotopoulos*
Department of Chemical Engineering, Princeton University, Princeton NJ 08544, USA
(Dated: February 6, 2008)

The global phase behavior of the lattice restricted primitive model with nearest neighbor exclusion has been studied by grand canonical Monte Carlo simulations. The phase diagram is dominated by a fluid (or charge-disordered solid) to charge-ordered solid transition that terminates at the maximum density, $\rho^*_{max} = \sqrt{2}$ and reduced temperature $T^* \approx 0.29$. At that point, there is a first-order phase transition between two phases of the same density, one charge-ordered and the other charge-disordered. The liquid-vapor transition for the model is metastable, lying entirely within the fluid-solid phase envelope.

I. INTRODUCTION

Recent theoretical and simulation studies of ionic systems have improved our understanding of their structure and thermodynamics[1,2,3,4,5,6,7,8]. One of the most successful and simplest ionic models is the restricted primitive model (RPM), in which the ions are viewed as equisized hard spheres carrying positive and negative charges of the same magnitude. The RPM exhibits vapor-liquid phase separation and the corresponding critical point was confirmed to belong to the three-dimensional Ising universality class[9,10].

The discretized version of the RPM, the lattice restricted primitive model (LRPM), has also been extensively studied by both simulation[11,12,13,14,15,16] and theoretical approaches[11,17,18,19,20,21,22]. In the LRPM, positions of the positive and negative ions of diameter σ are restricted to the sites of an underlying simple cubic lattice of spacing l; the parameter $\zeta = \sigma/l$ specifies how closely the lattice system approaches the continuum behavior. In addition to the obvious computational advantages[12], since the interactions between all lattice sites are pre-computed, the lattice model presents some unusual characteristics generally absent from non-ionic fluids[23]. For $\zeta = 1$, the most striking feature is an order-disorder transition[11,12], which is not present in the continuous version of the RPM. There is no gas-liquid transition and the coexistence is between a low-density disordered phase and an antiferromagnetically ordered high-density phase. The transition is continuous (Néel-type line) above and first-order below a tricritical point. However, for fine discretized lattices with $\zeta \geqslant 3$ the vapor-liquid coexistence is recovered and the critical point and coexistence curves converge to the values found in the continuum model for increasing values of ζ[10,12,24].

Several investigations have been performed of the $\zeta = 1$ LRPM with additional short-range attractions[14,17] or nearest-neighbor (nn) repulsions[15,18,19]. These models present a rich phase behavior as the nn strength is varied. For weak or vanishing nn interactions only order-disorder transitions and a tricritical point were found, while for increasing nn strength different scenarios could be possible, depending on the magnitude of the nn interaction. For short-range attractions both tricritical and gas-liquid critical points can become stable[14], while for nn repulsion the continuum-space behavior is recovered[15].

The present paper extends the previous study[15], of the LRPM model with variable nearest neighbor repulsion to the limit of infinite repulsion. The model is thus the lattice restricted primitive model with nearest neighbor exclusion (LRPM-nn). This is equivalent to a lattice restricted primitive model of discretization parameter $\zeta = \sqrt{2}$. Prior theoretical studies[18,19] with first, second and third nn exclusion indicate close similarity between the LRPM-nn phase diagram and the results for an off-lattice ionic system at high densities. Of particular interest to the present work are possible connections between order-disorder transitions and lower density vapor-liquid transitions and high density transitions between charge-ordered and charge-disordered phases[19]. The present paper is organized as follows. The model and computational details are given in Sec. II. Results are discussed in Sec. III. We close in Sec. IV with summary and conclusions.

II. MODEL AND SIMULATION METHODS

We consider a system of $2N$ charges, half of them carrying charge $+q$ and half charge $-q$, on a simple cubic lattice. We enforce nearest neighbor exclusion on the lattice and set the charge diameter as the unit of length, $\sigma = 1$. The lattice spacing is then $l = 1/\sqrt{2}$, such that the lattice discretization parameter[12] is defined as

*Corresponding author: azp@princeton.edu

$\zeta = \sigma/l = \sqrt{2}$. The charges interact through the (continuous space) Coulomb potential

$$U_{ij} = \frac{q_i q_j}{D r_{ij}} , \qquad (1)$$

where D is the dielectric constant of the structureless solvent in which the charges are immersed. While some studies of the phase behavior of the true lattice Coulomb potential are available[25], most prior studies of lattice RPM models have been done using the potential of equation (1).

Reduced quantities are defined as follows:

$$T^* = \frac{k_B T}{E_0}, \quad \rho^* = \frac{2N\sigma^3}{V}, \quad U^* = \frac{U}{E_0} , \qquad (2)$$

where σ is the ion diameter (taken as the unit of length), V is the volume of the system, U the energy per ion pair and $E_0 = q^2/D\sigma$ is the magnitude of Coulomb energy between two ions at close contact. The reduced chemical potential, μ^*, is defined so that at the limit of high temperatures and low densities, $\mu^* \to 2T^* \ln N\sigma^3/V$, where the factor 2 comes from the presence of two ions per minimal neutral "molecule" inserted or deleted in the simulations. With this choice of reduced units, the maximum density of the system at close packing is $\rho^*_{\max} = \sqrt{2}$.

The reduced box length, $L^* = L/\sigma$ is a non-integer quantity, as the lattice spacing is $l = 1/\sqrt{2}$; it is more convenient to use the lattice spacing as the reducing length in this case, so we define

$$L^\dagger = \frac{L}{l} = \sqrt{2}\frac{L}{\sigma} . \qquad (3)$$

The LRPM-nn model studied in the present work is equivalent to the limiting case of infinite repulsive coupling to nearest neighbor sites, $J \to \infty$, in the model studied in Ref.[15]. However, Ref.[15] used an effective charge diameter of $\sigma = \sqrt{2}$, so that reduced densities and temperatures are higher in the present study by factors of $2\sqrt{2}$ and $\sqrt{2}$, respectively. The unit conventions used here facilitate comparisons with previous studies of the LRPM model[12] and the continuous RPM[26,27].

Electrostatic interactions were computed using Ewald summation with conducting boundary conditions at infinity, 518 Fourier-space wave vectors and real-space damping parameter $\kappa = 5$. Interactions were precomputed at the beginning of the simulation runs for all possible pairs of lattice sites and stored in an array for computational efficiency.

We used grand canonical Monte Carlo (GCMC) simulations in cubic boxes subject to full periodic boundary conditions. Two types of moves were utilized, namely pair additions and removals and swapping of oppositely charged ions to enhance sampling of order-disorder transitions. To enhance acceptance of the insertion and removal steps we used distance-biased sampling, following Ref.[28]. Particle swaps constituted up to 60 % of attempted moves, depending on temperature and density.

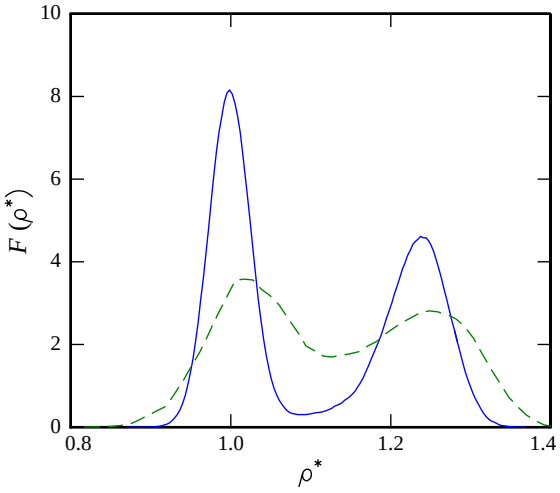

FIG. 1: (color online) Normalized density distribution, $F(\rho^*)$, at $T^* = 0.15$ in simulation boxes of size $L^\dagger = 12$ (continuous line) and $L^\dagger = 8$ (dashed line).

Multihistogram reweighting[24,29,30] techniques were used to analyze the simulation data. For the critical region we used mixed-field finite size scaling analysis proposed by Bruce and Wilding[31], which accounts for the lack of symmetry between coexisting phases in fluids. We did not attempt to incorporate corrections for pressure mixing in the scaling fields, as any such effects are expected to be small[32]. The Tsypin and Blöte[33] limiting distribution for the three-dimensional Ising model was used for obtaining the critical parameters. Typical runs involved 10^8 Monte Carlo steps for equilibration and 10^9 steps for production. Such runs required approximately 10 CPU hours on 3 GHz Pentium 4 processors. Longer runs were performed near the vapor-liquid critical point and at high densities at which the acceptance ratio for insertions and removals was lower. Statistical uncertainties were obtained from multiple independent runs with different pseudorandom sequences. The random number generator "ran2" of Ref.[34] was used for the calculations.

For the charge-disordered solid to charge-ordered solid part of the phase diagram (or "fluid"-solid), we were able to observe direct transitions between the ordered and disordered phases, as shown in Fig. 1. This established the relative free energies of the two phases and eliminated the need for thermodynamic integration to a reference state of known free energy. As seen in Fig. 1, for smaller boxes the probability of intermediate densities is greatly enhanced and the system readily passes between the two phases. For simulation boxes much greater than $L^\dagger = 12$, sampling is restricted to the phase from which the simulation is started; it is not possible to establish a reversible path from the charge-disordered solid (or fluid) to the charge-ordered solid phases using grand canonical simulations without umbrella sampling.

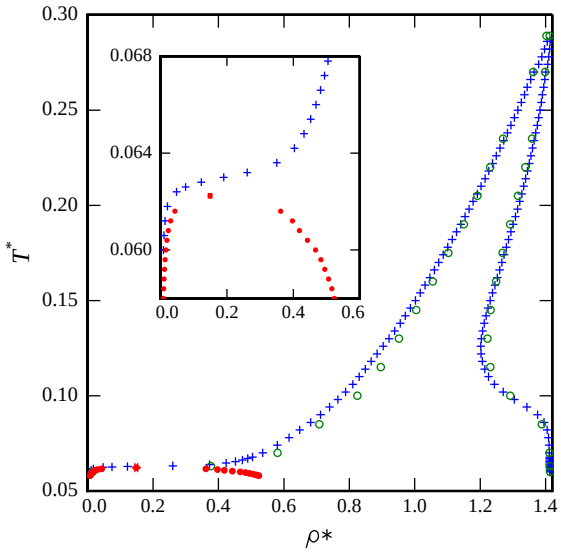

FIG. 2: (color online) Phase behavior of the LRPM-nn model. The "fluid"-solid transition is indicated by crosses ($L^\dagger = 12$) and open circles ($L^\dagger = 8$). Filled circles mark the vapor-liquid equilibrium phase boundaries obtained in a box of size $L^\dagger = 24$. The inset expands the region around the metastable vapor-liquid critical point. Statistical uncertainties are smaller than symbol size.

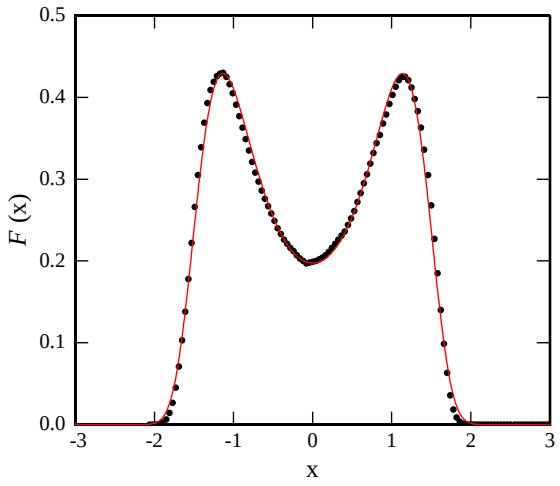

FIG. 3: (color online) . Order parameter distribution, $F(x)$, for a system of $L^\dagger = 24$ at conditions corresponding to the critical point listed in Table I. Points are simulation data and the line represents the analytical approximation of Ref.[33] for the three-dimensional Ising universality class limiting distribution. Simulation statistical uncertainties are comparable to symbol size.

III. RESULTS AND DISCUSSION

Fig. 2 shows the overall phase behavior for the LPRM-nn model. The "fluid"-solid transition dominates the phase diagram. It should be pointed out that the designation "fluid" is not appropriate at high densities. There is no first-order transition between fluid and solid phases in the $\sqrt{2}$ lattice hard sphere model to which the present model reduces at the limit of high temperatures. The $\sqrt{2}$ lattice hard sphere model has a second order transition at a density of $\rho^* \approx 0.59$[35,36], above which an fcc-ordered sublattice exists in the system. The lower-density phase for the LPRM-nn is a disordered fluid at lower temperatures but becomes increasingly solid-like at higher densities. Near the end-point of the transition the coexisting phases are both solids with face-centered-cubic overall arrangement of the particles, if one ignores the ion charge. For this reason, we enclose the term "fluid" in quotation marks when referring to the phase at the low-density side of this transition, to acknowledge the fact that the phase changes continuously from a disordered fluid to a charge-disordered solid.

The vapor-liquid envelope is seen in the inset to Fig. 2 to be metastable and wholly within the "fluid"-solid boundary. This is surprising for a system with long-range (Coulombic) interactions because the lack of a stable liquid phase is usually associated with *short-range* attractions[37]. This behavior can be rationalized by considering that the presence of the underlying lattice greatly stabilizes the solid, thus shifting the fluid-solid transition to higher temperatures. By contrast, for systems with very short range interactions, it is the destabilization of the liquid phase that leads to the disappearance of the vapor-liquid transition. The phase diagram for the LRPM-nn model is similar to that of the LRPM with $\zeta = 2$, obtained with large statistical uncertainties in Ref.[12] and studied theoretically in[20].

There is some system size dependence observed for the "fluid"-solid part of the phase diagram, especially at lower temperatures, as seen from the difference of the apparent phase boundaries. The smallest of the system sizes shown in Fig. 2 ($L^\dagger = 8$) can accommodate only 256 ions at full packing; it was included only for comparison purposes. The larger system ($L^\dagger = 12$) can accommodate 864 ions at close packing, but is still small enough to allow for efficient direct sampling of the order-disorder transition, as seen in Fig. 1.

The liquid-vapor critical point and phase coexistence envelope were obtained for system sizes ranging from $L^\dagger = 14$ to $L^\dagger = 24$. Because of the lower densities relative to the "fluid"-solid transition, larger systems were required. Results for the critical parameters are shown in Table I. The apparent (system-size dependent) critical temperature, T_c^*, chemical potential, μ_c^* and field mixing parameter $s_{\rm mix}^*$ were obtained by minimizing deviations between the universal order parameter distribution[33] and the observed distributions. A typical optimized order parameter distribution is shown in Fig. 3 , in which the abscissa is the mixed-field order parameter, $x = N(U^* - s_{\rm mix}^*)$. The estimates for the critical temperature do not vary significantly with system size, while the

TABLE I: Vapor-liquid critical parameters. Numbers in parentheses indicate statistical uncertainties in units of the last figure shown.

$L^\dagger$	T_c^*	μ_c^*	$s_{\rm mix}^*$	ρ_c^*
15	0.0623(1)	-1.5015(1)	-0.643(1)	0.132(1)
18	0.0624(1)	-1.5021(1)	-0.621(1)	0.155(2)
22	0.0622(1)	-1.5016(2)	-0.630(5)	0.150(4)
24	0.0622(1)	-1.5041(1)	-0.629(3)	0.148(3)

critical density first increases and then becomes slightly lower with system size.

These critical parameters can be compared with those for the related model of Ref.[15] with partial exclusion of nearest neighbor sites, $J = 0.3$, after taking into account the different reducing parameters. The $J = 0.3$ model has critical parameters (for $L^\dagger = 15$) $T_c^* = 0.0612(1)$, $\rho_c^* = 0.14(2)$, very similar to the LPRM-nn present model which corresponds to $J \to \infty$. However, the high-density (solid) phases of the two models are completely different, as discussed in the paragraphs that follow.

The critical temperature for the present model is slightly higher and the critical density significantly higher than the continuum RPM, for which $T_c^* = 0.04933(5)$, $\rho_c^* = 0.075(1)$[10]. Vapor-liquid critical parameters for models with $\zeta = 3$, 4 and 5 have been obtained in[12]; the critical temperatures and densities were found to be higher in coarser lattices, a trend consistent with the results of the present study.

At relatively high temperatures, Coulombic interactions become less important than excluded volume in determining the equation of state for the LPRM-nn model. At the limit of very high temperatures, we have already mentioned that the model is equivalent to a $\sqrt{2}$ lattice hard sphere model. At higher densities an fcc-ordered solid appears and at close packing every sphere occupies an ordered position. In LPRM-nn, the high-temperature solid is substitutionally disordered with respect to charge type. The continuous RPM model[26,27,38] has a transition from a charge-disordered to a charge-ordered solid phase at temperatures near $T^* \approx 0.29$. The fully occupied LPRM charge-ordered to charge-disordered phase transition has been investigated previously[13] and found to have a first order transition at the same temperature. The phase behavior of Fig. 1 has the same transition at a similar temperature range.

The structure of the ion-ordered solid is shown in Fig. 4. The structure is *P4/mmm* (tetragonal), identical to the "fcc"-ordered structure observed at high densities for the continuum RPM[26,27,38]. This structure has not yet been observed experimentally in systems of oppositely charged colloids[39].

In Ref.[40], the character of the transition between ordered and disordered solid phases for the continuous RPM was investigated using constant-pressure Monte Carlo simulations and found to be "weakly first order."

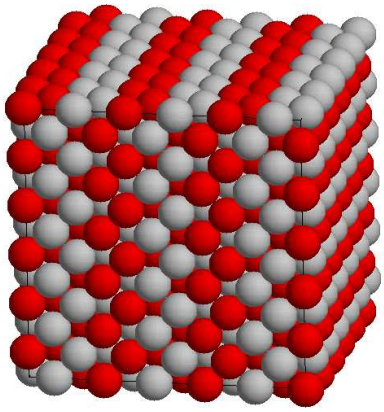

FIG. 4: (color online) Structure of the solid, $L^\dagger = 12$. Different shades (colors) represent oppositely charged ions.

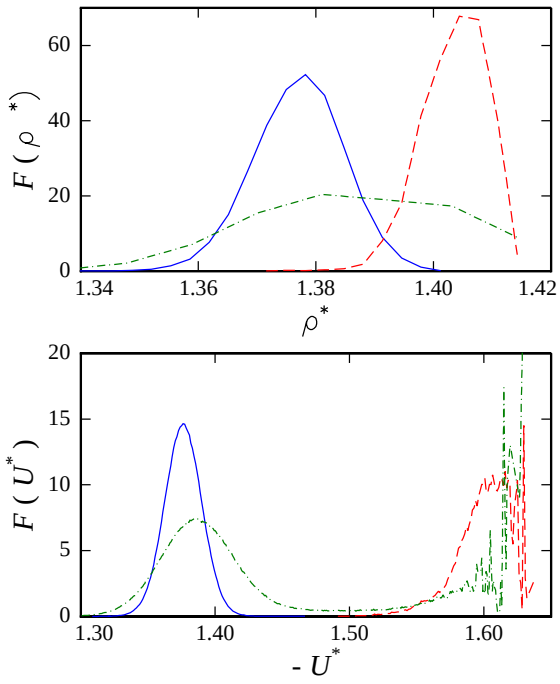

FIG. 5: (color online) Density (top) and energy (bottom) distributions, $F(\rho^*)$ and $F(U^*)$ at $T^* = 0.28$, $\mu^* = 0.8$. Solid line: $L^\dagger = 12$, started from disordered solid; dashed line: $L^\dagger = 12$, started from ordered solid; dash-dotted line: $L^\dagger = 8$.

For the LRPM-nn model, the densities of the coexisting phases (ordered and disordered solids) are seen in Fig. 2 to converge at the maximum density $\rho_{max}^* = \sqrt{2}$. Normalized probability distributions for the densities and energies are shown in Fig. 5 at $T^* = 0.28$ for two system sizes, $L^\dagger = 12$ and $L^\dagger = 8$. The apparent "noise" at low energies (to the right of the bottom part of the graph) is due to the finite number of states with one, two etc vacancies in the lattice model. For the smaller box, densities

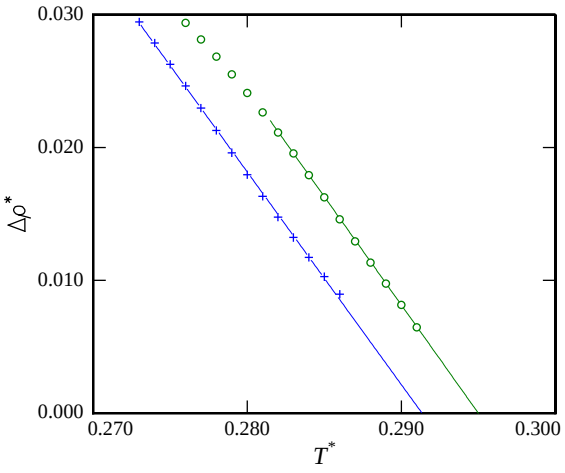

FIG. 6: (color online) Density difference between charged-ordered and charged-disordered phases for $L^\dagger = 12$ (crosses) and $L^\dagger = 8$ (open circles). Statistical uncertainties are comparable to symbol size. Lines are linear-least-squares fits to the points over the range indicated.

and energies corresponding to both phases are sampled in a single run. There is no hint of two peaks in the density distribution, but the energy distribution shows a clear separation of states into higher energy (less negative, disordered) and lower energies (ordered). For the larger box size, the simulations get trapped in the phase from which they are started; even though the density distributions of the two runs at identical chemical potentials overlap at $\rho^* \approx 1.39$, there is no overlap in the energy distributions.

We have computed the density difference between the charged-ordered and charged-disordered phases near the transition end-point by using energy (rather than density) to identify the phases. In other words, referring to Fig. 5, we collected the density under the charge-ordered (more negative energy) and charge-disordered (less negative energy) phases. The results allow us to extend the coexistence envelope to higher temperatures for which the density differences are small. The results for the density difference, $\Delta\rho^*$, as a function of temperature are shown in Fig. 6. The linear-least-squares fits to the points are indicated as lines in Fig. 6. These give in turn the temperature at which the first order transition occurs with *no density discontinuity*, as $T^* = 0.295(2)$ for $L^\dagger = 8$ and $T^* = 0.291(3)$ for $L^\dagger = 12$. At that limit, both coexisting phases are at the closed-packed density, $\rho^* = \rho^*_{max} = \sqrt{2}$. A fluid-solid phase transition with no density discontinuity has been established for the Gaussian core model[41]. Experimentally, several metallic elements, in particular Ce, Cs, Ba and Eu, have melting lines of zero slope in the pressure-temperature plane[42,43,44], also indicating a fluid-solid transition with no density discontinuity.

It is of interest to compare our results to the field-theoretic study of Ciach and Stell[19] for the LPRM-nn and to simulations of Abascal *et al.*[40] and Bresme *et al.*[26] for the continuous RPM at high densities. The main difference between our results and these prior studies is that we find that the charge-ordered and charge-disordered solids have a first-order transition with zero density difference at the closed-packed density. We speculate that such a transition may also be found in the continuous RPM near the close-packed density, as our findings seem to be generally consistent with those of Ref.[40].

IV. CONCLUSIONS

We have studied the phase diagram of the lattice restricted primitive model with nearest neighbor exclusion (LPRM-nn), using grand canonical Monte Carlo simulation and histogram reweighting techniques. The global phase diagram is dominated by the "fluid"-solid transition, which starts with a large density gap between a dilute gas phase and the solid at low temperatures. The transition ends at $T^* = 0.291(3)$ as a first order transition between charge-ordered and charge-disordered phases of the same density, $\rho^* = \sqrt{2}$. First-order transitions between phases of the same density in one-component systems have been observed for several metallic elements and for the Gaussian core model.

The liquid-vapor phase transition for the model was determined to be metastable, lying entirely within the "fluid"-solid phase envelope. The metastable critical point for the transition was obtained as $T^*_c = 0.0622(1)$, $\rho^*_c = 0.148(3)$, values higher than for the continuum RPM but consistent with previously determined trends for discretized lattice models.

While the broad outline of the phase diagram is consistent with theoretical predictions[19], our results differ from these predictions in some important aspects. In particular, the liquid / fcc-disordered transition is not present in our system. Our results are in near-quantitative agreement with calculations of ordered-disordered fcc phase transitions for the continuum RPM[40]. However, we find that the charge-ordered and charge-disordered phases maintain a first-order transition even though there is no density difference between the coexisting phases.

Acknowledgments

AD acknowledges financial support of the Brazilian agency CNPq - Conselho Nacional de Desenvolvimento Científico e Tecnológico. AZP acknowledges funding by the Department of Energy, Office of Basic Energy Sciences (through Grant No. DE-FG02-01ER15121) and ACS-PRF (Grant 38165 - AC9). We are grateful to Dr. Frank Stillinger for pointing out the existence of pure component systems that have first-order transitions with no density discontinuity. We also would like to thank

Dr. Alina Ciach, Dr. Carlos Vega, and Dr. Antti-Pekka Hynninen for helpful comments and discussions.

[1] Y. Levin, Rep. Prog. Phys. **65**, 1577 (2002).
[2] A. Z. Panagiotopoulos, J. Phys. Condens. Matter **17** S3205 (2005).
[3] M. E. Fisher, J.-N. Aqua and S. Banerjee, Phys. Rev. Lett. **95**, 135701 (2005).
[4] W. Zhou and J. K. Percus, Phys. Rev. Lett. **95**, 235701 (2005).
[5] Ciach A, Stell G, Int. J. Modern Phys. B **19**, 3309 (2005).
[6] A.-P. Hynninen and M. Dijkstra, J. Chem. Phys. **123**, 244902 (2005).
[7] J. M. Caillol, Molec. Phys. **103**, 1271 (2005).
[8] A.-P. Hynninen, M. Dijkstra and A. Z. Panagiotopoulos, J. Chem. Phys. **123**, 084903 (2005).
[9] E. Luijten, M. E. Fisher, and A. Z. Panagiotopoulos, Phys. Rev. Lett. **88**, 185701 (2002).
[10] Y. C. Kim and M. E. Fisher, Phys. Rev. Lett. **92**, 185703 (2004).
[11] R. Dickman and G. Stell, in *Simulation and Theory of Electrostatic Interaction in Solutions*, edited by L. R. Pratt and G. Hummer (AIP, Woodbury, 1999).
[12] A. Z. Panagiotopoulos and S. K. Kumar, Phys. Rev. Lett. **83**, 2981 (1999).
[13] N. G. Almarza and E. Enciso, Phys. Rev. E **64**, 042501 (2001).
[14] A. Diehl and A. Z. Panagiotopoulos, J. Chem. Phys. **118**, 4993 (2003).
[15] A. Diehl and A. Z. Panagiotopoulos, Phys. Rev. E **71**, 046118 (2005).
[16] K. Hoang, K. Desai,S. D. Mahanti, Phys. Rev. B **72**, 064102 (2005).
[17] A. Ciach and G. Stell, J. Mol. Phys. Liq. **87**, 255 (2000); J. Chem. Phys. **114**, 382 (2001); *ibid* **114**, 3617 (2001); Physica A **306**, 220 (2002).
[18] A. Ciach and G. Stell, Phys. Rev. Lett. **91**, 060601 (2003).
[19] A. Ciach and G. Stell, Phys. Rev. E **70**, 016114 (2004).
[20] A. Ciach, Phys. Rev. E **70**, 046103 (2004).
[21] S. Moghaddam, Y. C. Kim and M. E. Fisher, J. Phys. Chem. B **109**, 6824 (2005).
[22] M. N. Artyomov and A. B. Kolomeisky, Mol. Phys. **103**, 2863 (2005).
[23] A. Z. Panagiotopoulos, J. Chem. Phys. **112**, 7132 (2000).
[24] A. Z. Panagiotopoulos, J. Chem. Phys. **116**, 3007 (2002).
[25] V. Kobelev, A. B. Kolomeisky and A. Z. Panagiotopoulos, Phys. Rev. E **68**, 066110 (2003).
[26] F. Bresme, C. Vega and J. L. F. Abascal, Phys. Rev. Lett. **85**, 3217 (2000).
[27] C. Vega, J. L. F. Abascal, C. McBride and F. Bresme, J. Chem. Phys. **119**, 964 (2003).
[28] G. Orkoulas and A. Z. Panagiotopoulos, J. Chem. Phys. **101**, 1452 (1994).
[29] A. M. Ferrenberg and R. H. Swendsen, Phys. Rev. Lett. **61**, 2635 (1988); **63**, 1195 (1989).
[30] D. Frenkel and B. Smit, *Understanding Molecular Simulation* (Academic, New York, 1996).
[31] A. D. Bruce and N. B. Wilding, Phys. Rev. Lett. **68**, 193 (1992); N. B. Wilding and A. D. Bruce, J. Phys.: Condens. Matter **4**, 3087 (1992).
[32] Y. C. Kim and M. E. Fisher, J. Phys. Chem. B **108**, 6750 (2004); M. E. Fisher and G. Orkoulas, Phys. Rev. Lett. **85**, 696 (2001).
[33] M. M. Tsypin and H. W. J. Blöte, Phys. Rev. E **62**, 73 (2000).
[34] W. H. Press, S. A. Teukolsky, W. T. Vetterling, and B. P. Flannery, *Numerical Recipes in FORTRAN*, 2nd ed. (Cambridge University Press, Cambridge, 1992).
[35] A. Z. Panagiotopoulos, J. Chem. Phys. **123**, 104504 (2005).
[36] D. S. Gaunt, J. Chem. Phys. **46**, 3237 (1967).
[37] P. R. ten Wolde and D. Frenkel, Science **277**, 1975 (1997).
[38] C. Vega, F. Bresme and J.L.F. Abascal, Phys. Rev. E **54**, 2746 (1996).
[39] A.-P. Hynninen, M. E. Leunissen, A. van Blaaderen and M. Dijkstra, Phys. Rev. Lett. **96**, 018303 (2006).
[40] J. L. F. Abascal, C. Vega, C. McBride and F. Bresme, Phys. Rev. E **68**, 052501 (2003).
[41] S. Prestipino, F. Saija and P. V. Giaquinta, Phys. Rev. E **71**, 050102 (2005).
[42] G. C. Kennedy, A. Jayaraman, and R. C. Newton, Phys. Rev. **126**, 1363 (1962).
[43] A. Jayaraman, W. Klement, and G. C. Kennedy, Phys. Rev. Lett. **10**, 387 (1963).
[44] A. Jayaraman, Phys. Rev. **137**, A179 (1965).